Supporting Information

for *Biomacromolecues*

Cooperative Catechol-Functionalized Polypept(o)ide Brushes and Ag Nanoparticles for the Combination of Protein Resistance and Antimicrobial Activity on Metal Oxide Surfaces

Jin Yoo, [†] *Alexander Birke,*[‡] *Joonwon Kim,*[§] *Yeongseon Jang,*[#] *Seukyoung Song,*[¶] *Seungmi Ryu,*[¶] *Byung-Soo Kim,*[¶] *Byung-Gee Kim,*[§] *Matthias Barz*[‡,]* * and Kookheon Char*[†,]* *

[†]The National Creative Research Initiative Center for Intelligent Hybrids, School of Chemical and Biological Engineering, Seoul National University, Seoul 08826, Republic of Korea, [‡]Institute of Organic Chemistry, Johannes Gutenberg-University Mainz, Duesbergweg 10-14, 55128 Mainz, Germany, [§]Institute of Molecular Biology and Genetics, School of Chemical and Biological Engineering, Seoul National University, Seoul 08826, Republic of Korea, [#]School of Chemical and Biomolecular Engineering, Georgia Institute of Technology, Atlanta, GA 30332, USA, [¶]Interdisciplinary Program for Bioengineering, School of Chemical and Biological Engineering, Seoul National University, Seoul 08826, Republic of Korea,

*Matthias Barz, Ph.D., E-mail: barz@uni-mainz.de

*Kookheon Char, Ph.D., E-mail: khchar@snu.ac.kr

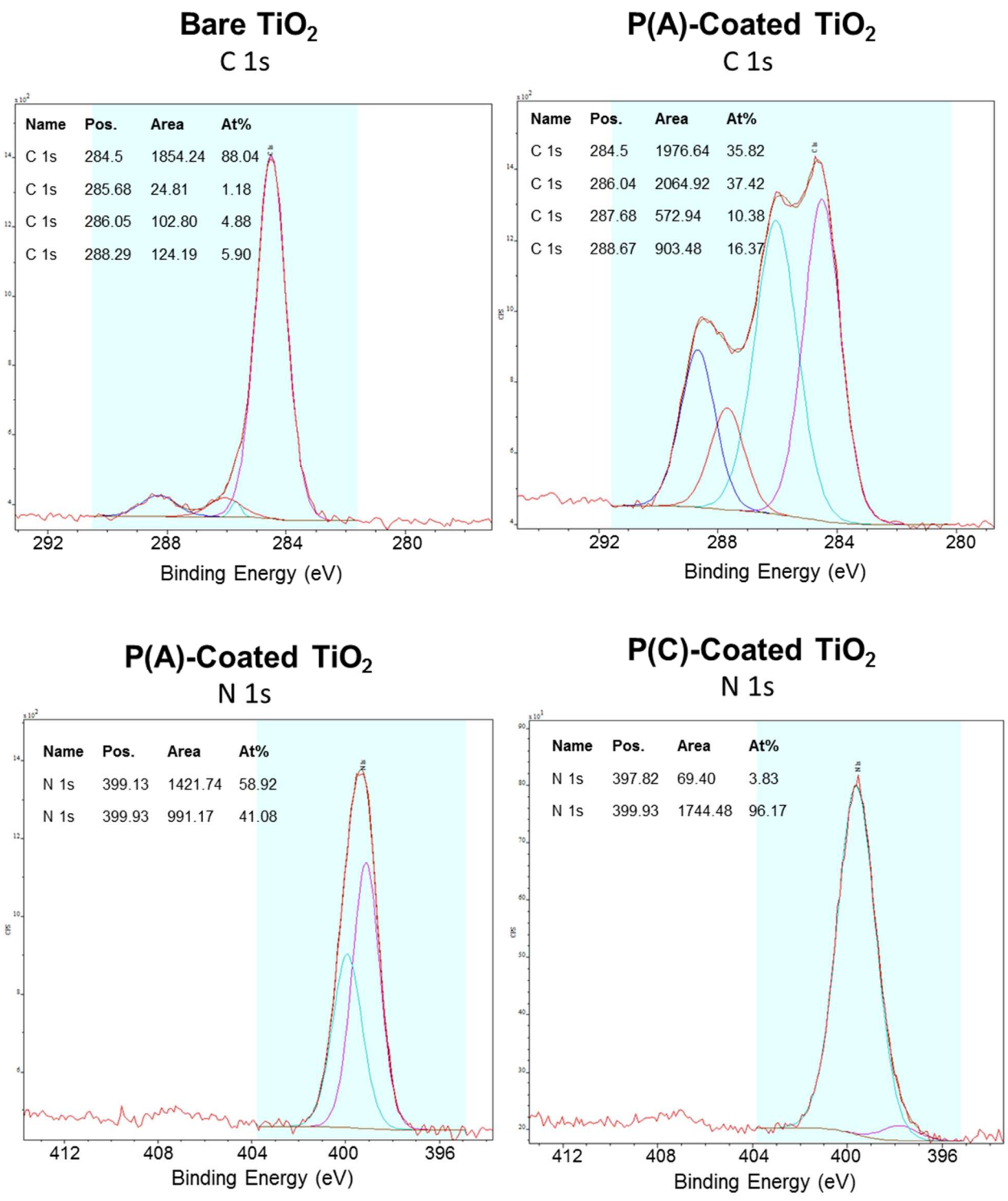

Figure S1. XPS deconvoluted peaks in the high resolution spectra of bare and polypept(o)ide-coated surfaces.

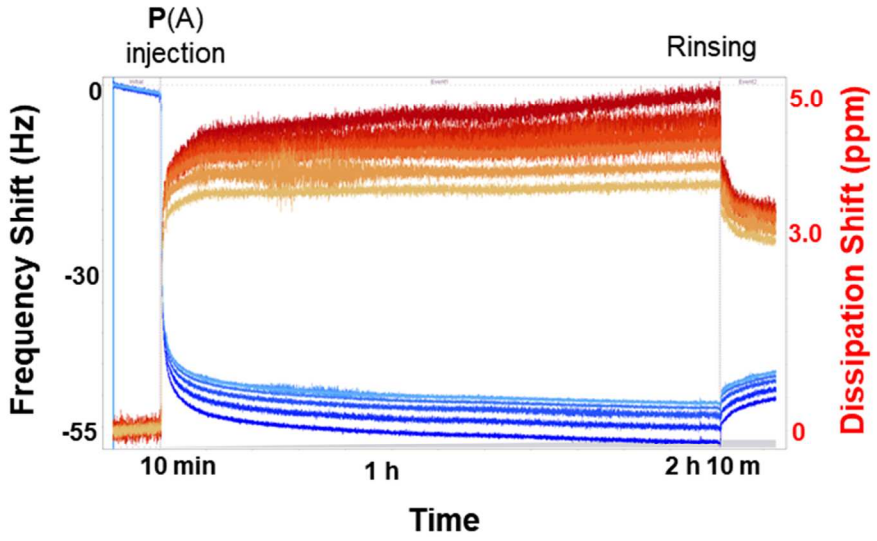

Figure S2. QCM-D data of the adsorption of **P**(A) on TiO_2 surface. Frequency shift normalized by overtone number is indicated in blue graphs, and the dissipation factor shift is marked as red. Remarkable overtone-dependence and high dissipation shift were found upon adsorption, suggesting the formation of soft and dissipative polymer layers.

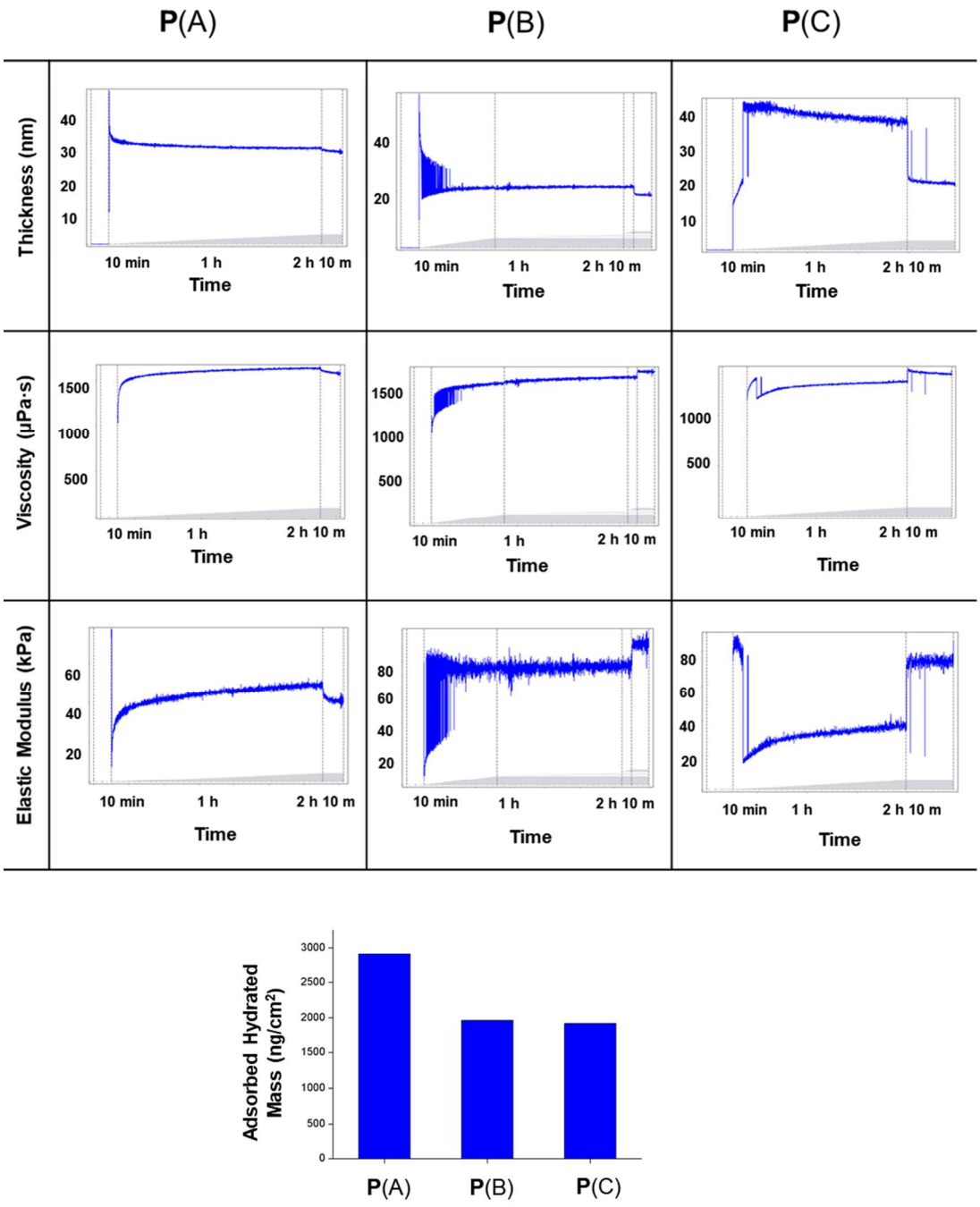

Figure S3. Brush layer information obtained by Q-sense Dfind software.

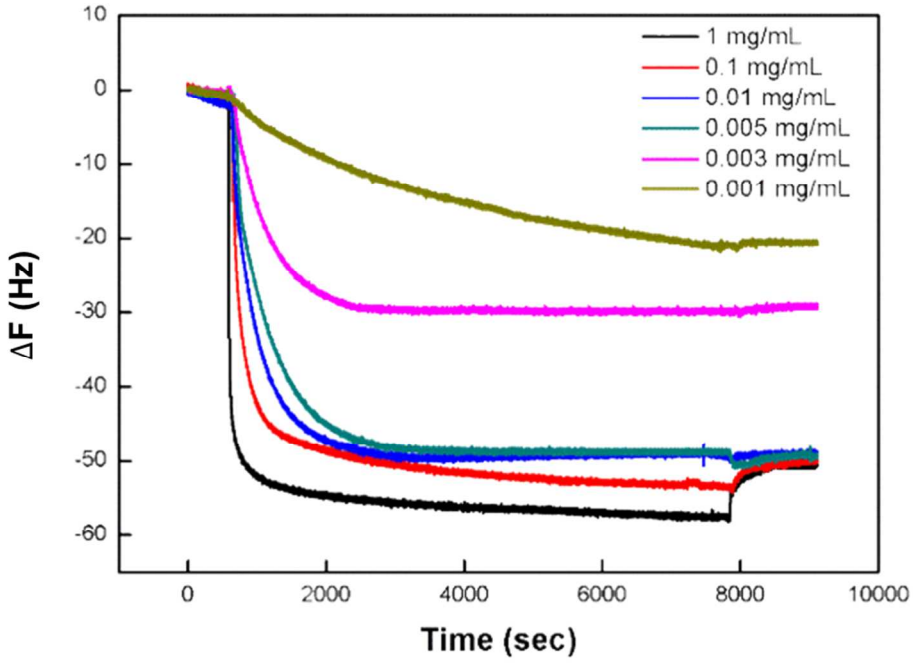

Figure S4. Adsorption of **P**(A) to titanium oxide surface corresponding to concentration of **P**(A) solution was measured by QCM-D.

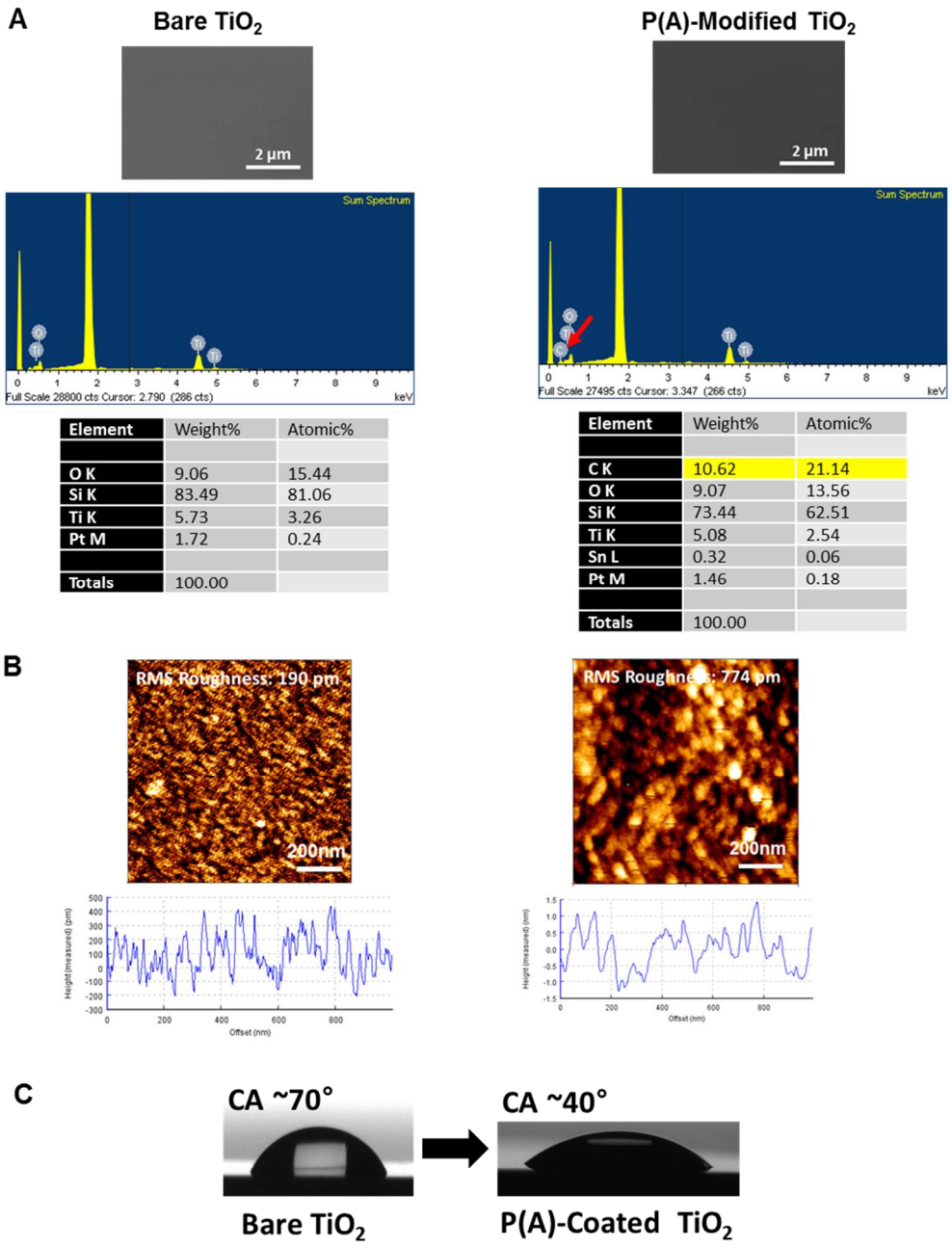

Figure S5. Surface characterization and comparison of **P**(A)-modified surfaces and bare surfaces. (A) EDS analysis showing existence of carbon on **P**(A)-modified surfaces. (B) Surface morphology and roughness changes in polymer coated TiO_2. (C) Contact angle measurements of bare and **P**(A)-coated surfaces.

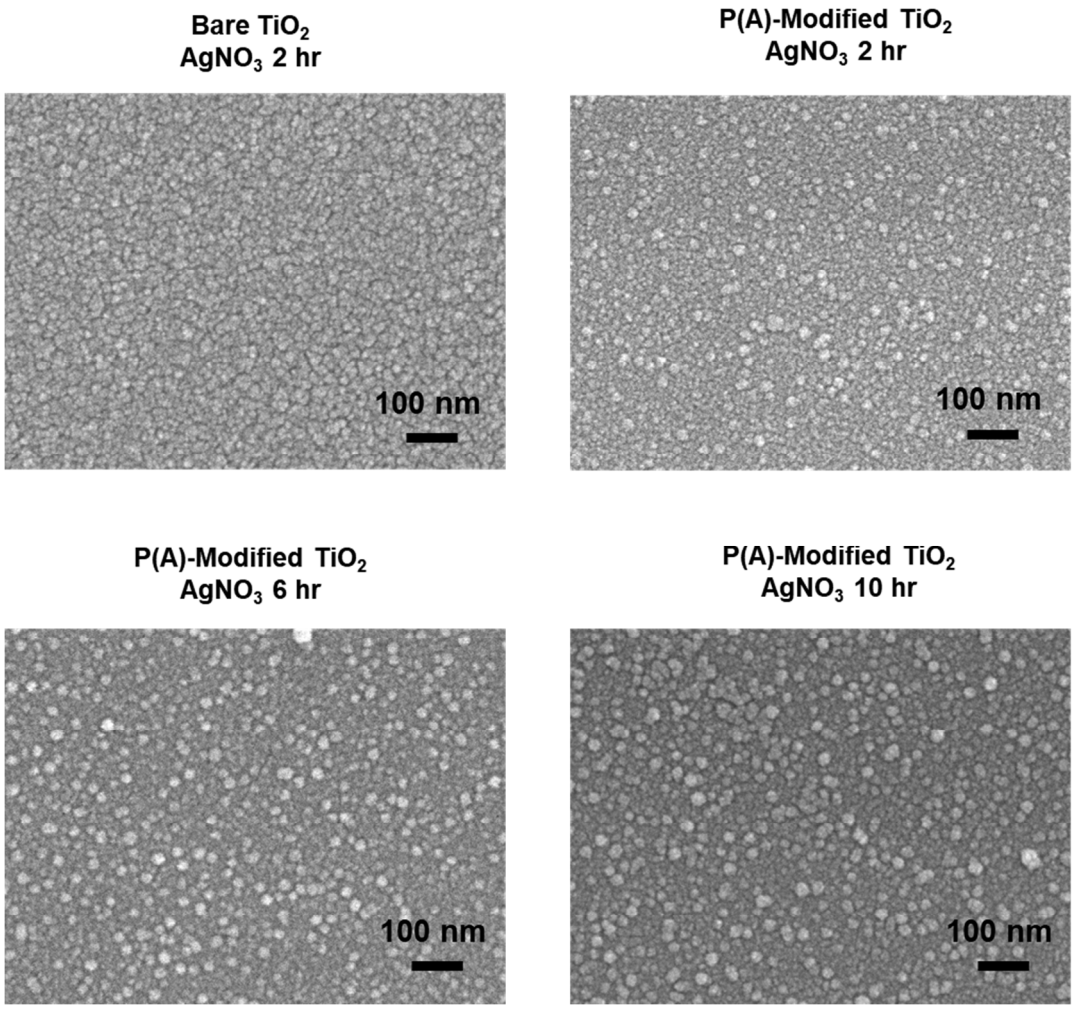

Figure S6. Surface characterization of Ag NP-conjugated surfaces with different immersion time in $AgNO_3$ solution. We note that, without **P**(A) functionalization, Ag NP formation was not possible due to the absence of reductants originating from **P**(A).

.

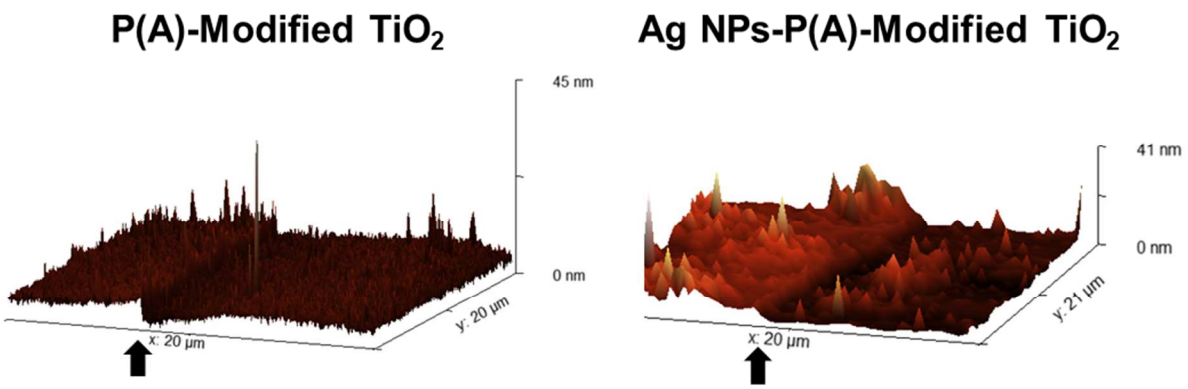

	Dry Thickness (nm)
P(A)-Modified TiO_2	4.52±0.46
Ag NPs-P(A)-Modified TiO_2	6.95±1.14

Figure S7. The film thicknesses of **P**(A)-coated surfaces and Ag NPs-modified **P**(A) surfaces measured by AFM.

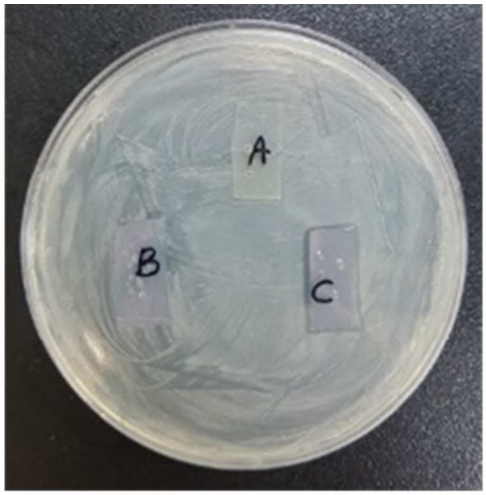

A: Bare TiO_2
B: P(A)-Modified TiO_2
C: Ag NPs-P(A)-Modified TiO_2

Figure S8. Inhibition zones of the growth of *E.coli* samples. Ag NPs-**P**(A)-modified TiO_2 substrates shows slightly enhanced inhibition zones around the substrate as well as antibacterial activity of the surface.

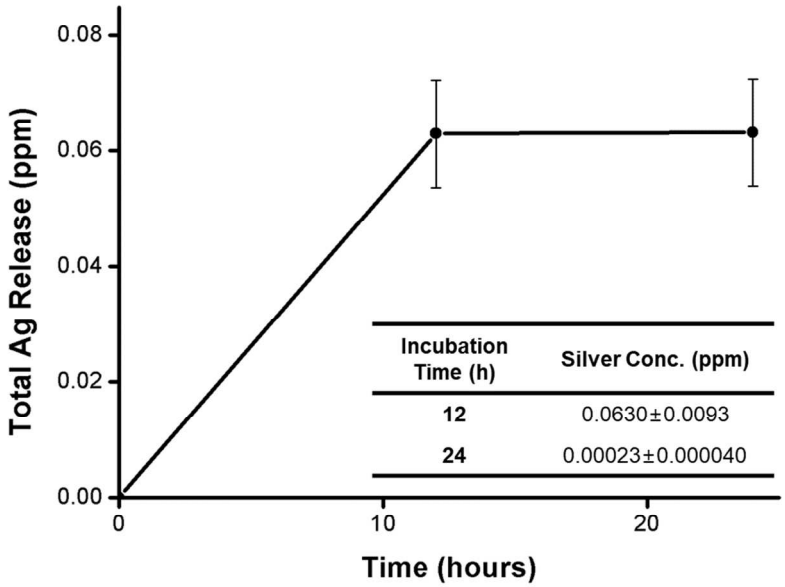

Figure S9. The cumulative silver ion release of an Ag NP-**P**(A)-modified TiO_2 surface and noncumulative silver release (inner table) in typical physiological environment. In general, Ag NPs follow the following redox reaction and release silver ions.[1]

$$2Ag(s) + 1/2O_2(aq) + 2\ H^+(aq) \leftrightarrow 2Ag^+(aq) + H_2O(aq)$$

It is believed that, as the glutamic acid block has negative charges in physiological environment, silver ions showed the slow-release over the long period (12 hours).

1. Jo, Y. K.; Seo, J. H.; Choi, B. H.; Kim, B. J.; Shin, H. H.; Hwang, B. H.; Cha, H. J., Surface-Independent Antibacterial Coating Using Silver Nanoparticle-Generating Engineered Mussel Glue. *Acs Appl Mater Inter* **2014,** *6* (22), 20242-20253.